Kinetics of the Coil−Globule Transition of Poly(methyl methacrylate) in a Mixed Solvent

Yoshiki Nakamura, Naoki Sasaki, and Mitsuo Nakata*

Department of Polymer Science, Faculty of Science, Hokkaido University, Kita-ku, Sapporo 060-0810, Japan

Received January 12, 2001; Revised Manuscript Received May 17, 2001

ABSTRACT: The coil−globule transition and chain collapse process were studied for poly(methyl methacrylate) in the mixed solvent *tert*-butyl alcohol + water (2.5 vol %) by static light-scattering measurements. The expansion factor α^2 for the mean-square radius of gyration was obtained as a function of time for various molecular weights. For the molecular weights $M_w \times 10^{-6} = 1.57$, PMMA chains collapsed to an equilibrium globule within 30 min after quench. For $M_w \times 10^{-6} = 4.0$ and 12.2, chain collapse processes were observed for time periods of hours and days, respectively. The time dependence of the observed expansion factor was represented by the stretched exponential form $\alpha^2 = \alpha^2_\infty + (1 - \alpha^2_\infty) \exp[-(t/\tau^*)^\beta]$, where α^2_∞ is the equilibrium expansion factor sufficiently long time after quench. β was obtained in the range from 0.1 to 0.4 and decreased with decreasing temperature and increasing molecular weight. From the behavior of β, the stretched exponential process was suggested to be intrinsic to each polymer chain rather than due to a superposition of exponentially collapse processes of polymer chains with various decay times. The equilibrium expansion factor obtained as a function of temperature and molecular weight was represented by the theoretical prediction $\alpha^3 - \alpha - C(\alpha^{-3} - 1) = B(1 - \theta/T)M^{1/2}$. The constants B and C were determined to be $B = 0.0164$ and $C = 0.049$ independent of the molecular weight.

1. Introduction

The coil−globule transition is a phenomenon characteristic of linear polymer chain and provides an insight into a conformational transition of biopolymers and a volume transition of polymer chain network.[1,2] Since Stockmayer[3] predicted collapse of polymer chain, many theoretical[4−10] and experimental studies[11−23] have been made to elucidate the equilibrium properties of the coil−globule transition. The polymer chain size in a globule region was explored for specific systems and/or under extreme conditions by light-scattering experiments and compared with theoretical predictions. For kinetics of the coil−globule transition, de Gennes first argued the mechanism of chain collapse and proposed a two-stage process based on a phenomenological model.[24] Grosberg et al. argued that the polymer chain shrinks in a self-similar manner due to crumpling in the first stage and the crumpled globule contracts to an equilibrium globule by means of reptation-like motion in the second process.[25,26] Further understanding of the chain collapse process was put forward by computer simulations[27−30] and by analyses with phenomenological models.[31,32] By Monte Carlo simulation Kuznetsov et al. visualized a chain collapse process with snapshots of transient chain conformations and predicted a three-stage collapse process.[29]

de Gennes estimated the characteristic time to be of order 10^{-3} s for the first stage of chain collapse.[24] Although this small characteristic time was unfavorable for an experimental observation of collapse process, Chu et al. carried out dynamic light-scattering measurements on a dilute solution of polystyrene with the molecular weight $M_w = 8.1 \times 10^6$ at the concentration 8.7×10^{-6} g/cm^3 and suggested a two-stage collapse process with the characteristic times of 357 and 323 s in the first and second stages, respectively.[33,34] Wu and Zhou observed a chain collapse process for poly(*N*-isopropylacrylamide) (PNIPAM) with $M_w = 1.08 \times 10^7$ in water by measuring hydrodynamic radius.[35] When the solution, which had the phase transition temperature near 32.00 °C, was quenched from 30.59 to 31.82 °C, a two-stage collapse process was observed with the characteristic time 50 s for the first stage and 300 s for the second stage. When quenched to 33.02 °C, the chain collapse was too fast to be followed. Zhu et al. prepared latex particles coated by PNIPAM and measured the overall hydrodynamic diameter in the presence of sodium dodecyl sulfate.[36,37] When the solution was quenched into a collapse region for PNIPAM, they observed a contraction process of the overall diameter for a time period of several hours. The contraction process was caused by a conformational change of PNIPAM chains at the interface and compared with a computer simulation.[29]

Previously, we studied the processes of the chain collapse[38] and chain aggregation[39,40] for dilute solutions of poly(methyl methacrylate) in isoamyl acetate by static light-scattering experiments. For $M_w \times 10^{-6} = 8.4$ and 12.2, we determined the mean-square radius of gyration $\langle s^2 \rangle$ of the polymer chain as a function of time after the quench of solution. The collapse of the PMMA chain to an equilibrium globule was found to require a time period of a few thousand minutes. The expansion factor α^2 ($= \langle s^2 \rangle / \langle s^2 \rangle_0$) as a function of time was represented by a power law with an exponent near $^1/_2$ and was extrapolated smoothly to the initial state of $\alpha^2 = 1$ at $t = 0$, though the measurements of $\langle s^2 \rangle$ were started 30 min after quench because of a blank time for a temperature equilibration. This behavior of α^2 suggested a single-stage chain collapse.

For $M_w \times 10^{-6} = 2.35$ and 4.4, we observed a very slow cluster formation of polymer chains in the phase separation process after quench.[39,40] The clusters grew exponentially, indicating a reaction-limited cluster ag-

10.1021/ma010063h CCC: $20.00
Published on Web 07/11/2001

gregation (RLCA).[41] Since the cluster formation occurs through a reaction between polymer segments, the slow phase separation may have an intimate correlation with the slow chain collapse. Thus, the kinetics of chain collapse as well as chain aggregation may be dominated by a specific nature of the system. On the other hand, the size of a fully collapsed chain is determined by the second and third virial coefficients for segment interactions. We demonstrated that the equilibrium globule in the mixed solvent of *tert*-butyl alcohol + water at 2.5 vol % of water was much more compact than that in isoamyl acetate.[19] It is interesting to reveal the chain collapse process to such a compact globule.

In this study, kinetics of chain collapse was investigated for PMMA in the mixed solvent *tert*-butyl alcohol + water (2.5 vol %) with various molecular weights by static light scattering. For $M_w \times 10^{-6} = 1.57$ and 2.84, polymer chains contracted to equilibrium globules within about 30 min after quench. For $M_w = 12.2 \times 10^6$ the chain collapse process was observed for a long time period from a day to weeks depending on the quench depth. The expansion factor $\alpha^2(t)$ in the chain collapse process was analyzed as a function of time with an equilibrium expansion factor α^2_∞ obtained sufficiently long time after quench. The time dependence of $\alpha^2(t)$ was represented by a stretched exponential function in the whole time period irrespective of the quench depth with an exception at a final stage at deep quench depth, say, in the range $\alpha^2 < 0.1$. Since the stretched exponential functions could be fitted to the data of $\alpha^2(t)$ under the initial condition of $\alpha^2(0) = 1$, the contraction process in the range $\alpha^2 > 0.1$ appeared to be a single-stage collapse process.

2. Experimental Section

Sample and Solution Preparation. In a previous study,[18] PMMA was prepared by bulk polymerization of the monomer and separated into 16 fractions (series M19) by a fractional solution method. In this study, light-scattering measurements were performed for the sixth M19-F6, the ninth M19-F9, and the twelfth fraction M19-F12 with the molecular weight $M_w \times 10^{-6} = 1.57$, 2.84, and 4.0, respectively. As a sample of very high molecular weight, the ninth fraction M21-F9 with $M_w = 12.2 \times 10^6$ from a different fraction series M21 was used as in a previous study.[38] The molecular weight distribution has been estimated as $M_w/M_n \sim 1.20$ for the samples. *tert*-Butyl alcohol was fractionally distilled immediately before use. Water was purified by a standard method. As a solvent for PMMA, we prepared the mixed solvent *tert*-butyl alcohol (1) + water (2) at the volume fraction $u_2 = 0.025$ of water.

For light-scattering measurements, PMMA solutions were made at four concentrations near c (10^{-4} g/cm^3) = 1.2, 2.5, 3.8, and 5.2 for $M_w \times 10^{-6} = 1.57$ and 2.84 and near c (10^{-4} g/cm^3) = 0.7, 1.3, 1.9, and 2.6 for $M_w \times 10^{-6} = 4.0$ and 12.2. Each solution was transferred into an optical cell of 18 mm i.d. and 1 mm wall thickness and sealed tightly with a Teflon cap to prevent evaporation of the solvent and kept under the saturated vapor of the mixed solvent at the θ-temperature 41.5 °C in the dark. Optical clarification of the solutions for $M_w \times 10^{-6} = 1.57$, 2.84, and 4.0 was made with a Sartorius membrane filter (SM 116, 0.45 or 0.8 μm). The solutions for $M_w = 12.2 \times 10^6$ were kept still for a few days to sediment impurity particles to the bottom in the cell, which made optical clarification effectively for the solutions of very high molecular weight.

Static Light Scattering. The light-scattering measurement was carried out at an angular interval of 15° in the range from 30° to 150° with unpolarized incident light at 435.8 nm of a mercury arc as described elsewhere.[19] Light-scattering measurements were carried out in the temperature range from 20 to 55 °C. The optical cell kept at the θ-temperature was immersed in a thermostated cylindrical cell at the center in the photometer, and the measurement of scattered light was started 30 min after the setup of the cell on account of thermal equilibration. For $M_w = 12.2 \times 10^6$, measurements on a chain collapse process at a temperature required very long time period of a few months. In this case, the optical cells were kept at the constant temperature under the saturated vapor of the mixed solvent in a thermostated water bath and were transferred occasionally to the cylindrical cells in the photometer for measurement.

The mixed solvent *tert*-butyl alcohol (1) + water (2) at the volume fraction $u_2 = 0.025$ of water behaved as a single solvent in the light-scattering experiment because of vanishing derivative $dn/du_2 = 0$ of the refractive index n of the solvent near $u_2 = 0.025$, though the refractive index difference between the alcohol and water was not small. u_2 denoted the volume fraction of the alcohol in a previous study.[18] The refractive index increment dn/dc (cm^3/g) at each temperature t (°C) was evaluated from the relation $dn/dc = 0.0994 + 3.2 \times 10^{-4}t$ obtained for the mixed solvent in the previous study.

To determine M_w, $\langle s^2 \rangle$, and the second virial coefficient A_2, the light-scattering data at an angle θ were transformed to the excess Raylaigh ratio R_θ and analyzed by the scattering equation[42]

$$(Kc/R_\theta)^{1/a} = M_w^{-1/a}\{1 + (1/3a)\langle s^2 \rangle q^2 + (2/a)M_w A_2 c\} \quad (1)$$

with $K = (2\pi^2 n^2/N_A\lambda^4)(dn/dc)^2$ and $q = (4\pi n/\lambda)\sin(\theta/2)$, where N_A is Avogadro's number and λ is the wavelength of incident light in a vacuum. The constant a in the exponent was introduced for a convenience of experimental data analysis. In a practical data analysis, an appropriate value of a should be employed depending on the maximum value of $\langle s^2 \rangle q^2$. We used $a = 2.0$ for $M_w \times 10^{-6} = 1.57$, 2.84, and 4.0 and $a = 1.5$ for $M_w = 12.2 \times 10^6$ to obtain straight lines in the plot of $(Kc/R_\theta)^{1/a}$ vs $\sin^2(\theta/2)$.

Phase Separation Temperature. To determine the phase separation temperature, we prepared solutions in the same concentration range as in the case of the light-scattering measurement. The temperature of the solutions was lowered by 0.1 K stepwise. At each step scattered intensity at an angle 30° was monitored for a few days or more because of a long lag period for an appearance of incipient phase separation. The phase separation temperature T_p was determined as the temperature at which an increase of scattered intensity was detected. However, for $M_w = 12.2 \times 10^6$, T_p could not be determined by this method because of an extremely long lag period. Thus, T_p (c 10^{-4} g/cm^3) at each concentration was determined to be 35.7 °C (1.43), 36.2 °C (2.73), 36.6 °C (4.17), and 36.7 °C (5.58) for $M_w = 1.57 \times 10^6$, 36.5 °C (1.24), 37.0 °C (2.47), 37.2 °C (3.73), and 37.4 °C (5.00) for $M_w = 2.84 \times 10^6$, and 36.7 °C (0.62), 37.2 °C (1.29), 37.4 °C (1.96), and 37.7 °C (2.56) for $M_w = 4.0 \times 10^6$. The above phase separation temperatures show small dependences on the molecular weight and concentration, and T_p for $M_w = 12.2 \times 10^6$ was conjectured to be below 39.0 °C by a direct extrapolation.

3. Experimental Results

Analysis of Light Scattering Data. Figure 1 shows the Zimm plots of light-scattering data for $M_w = 12.2 \times 10^6$ according to eq 1 with $a = 1.5$. Plots a and b were obtained 30 min after quench to the θ-temperature 41.5 and 20.0 °C, respectively. For each of the plots a and b, the straight lines given for the dependence of $(Kc/R_\theta)^{1/1.5}$ on $\sin^2(\theta/2)$ have a same slope and are extrapolated to $\theta = 0$ as shown by the filled circles. $\langle s^2 \rangle$ was estimated from the slope of the parallel straight lines. M_w and A_2 were estimated from the intercept and slope of the straight line for the filled circles, respectively. The parallel lines and common intercept shown in Figure 1 allowed us to determine M_w and $\langle s^2 \rangle$ reliably. The single plot c was obtained for the solution at the highest concentration 150 min after the quench to 20.0 °C. The

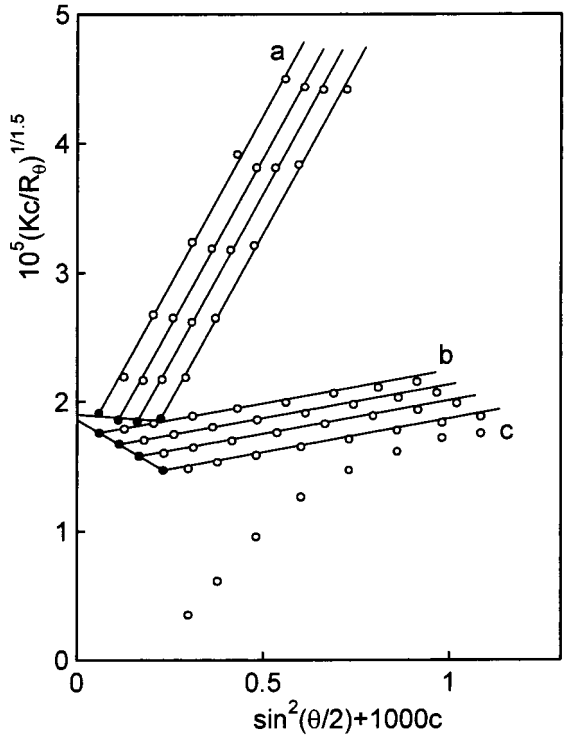

Figure 1. Zimm plot of $(Kc/R_\theta)^{1/1.5}$ as a function of $\sin^2(\theta/2)$ and c (g/cm^3) for light-scattering data of PMMA in the mixed solvent *tert*-butyl alcohol + water (2.5 vol %) with $M_w = 12.2 \times 10^6$. Plots a and b were obtained 30 min after quench to 41.5 and 20.0 °C, respectively. Single plot c was obtained 150 min after quench to 20.0 °C at the highest concentration.

marked behavior at smaller angles is caused by strong forward scattering due to the incipient phase separation. Plots of $(Kc/R_\theta)^{1/1.5}$ vs $\sin^2(\theta/2)$ at the two lowest concentrations at 20.0 °C were parallel with each other for several hours after the quench and yielded the correct molecular weight and very slow decrease of $\langle s^2 \rangle$. The plot at the lowest concentration yielded a straight line for a few months and used to pursue the decrease of $\langle s^2 \rangle$. Since, at temperatures above 20.0 °C, the effect of phase separation was negligibly small even at the highest concentration, M_w and $\langle s^2 \rangle$ were determined by the Zimm plot composed of data at four concentrations.

Figure 2 shows the example of the Zimm plot for $M_w = 12.2 \times 10^6$. Plots a and b were obtained 30 and 178 560 min (4 months) after quench to 23.0 °C, respectively. The plot at 178 560 min does not seem to be affected by an effect of phase separation and, in fact, yields the molecular weight correctly as $M_w = 13.1 \times 10^6$. Accordingly, $\langle s^2 \rangle$ was estimated accurately from the slope of the parallel lines for $(Kc/R_\theta)^{1/1.5}$ vs $\sin^2(\theta/2)$. In this way, $\langle s^2 \rangle$ was determined at various times between 30 and 178 560 min after the quench.

Since the filled circles extrapolated to $\theta = 0$ in Figures 1 and 2 yield the straight lines with well-defined slopes, the second virial coefficient A_2, though apparent one far below the θ-temperature, can be determined unambiguously. From observed values of A_2, the θ-temperature of the present system was determined to be 41.5 °C, which agreed with the value obtained in the previous study.[18] At the θ-temperature we estimated $\langle s^2 \rangle_0 \times 10^{11} = 0.96$, 1.76, 2.57, and 8.19 cm^2 and characteristic ratio $\langle s^2 \rangle_0 / M_w \times 10^{18} = 6.1$, 6.2, 6.4, and 6.7 cm^2 for $M_w \times 10^{-6} = 1.57$, 2.84, 4.0, and 12.2, respectively. These values of the characteristic ratio agreed with previous values.[38]

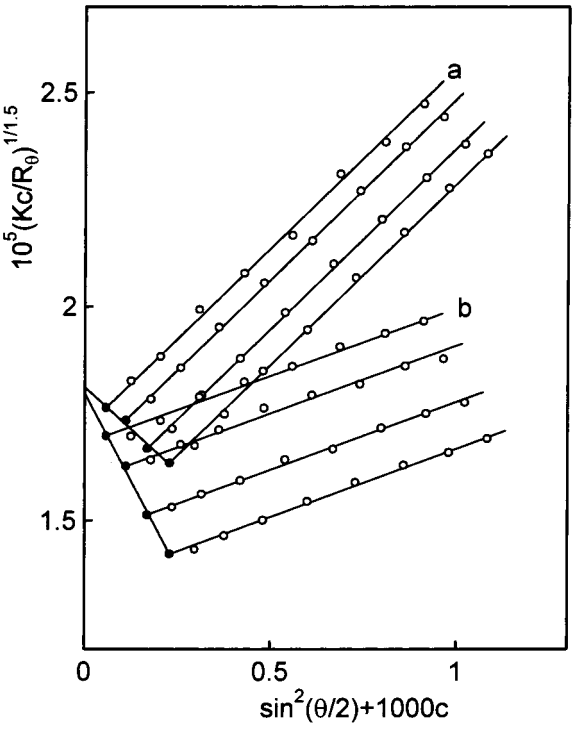

Figure 2. Zimm plot of light-scattering data for the same solution as in Figure 1. Plots a and b were obtained 30 and 178 560 min after quench to 23.0 °C, respectively.

Expansion Factor Determined 30 min after Quench. The values of $\langle s^2 \rangle$ and A_2 at 30 min after quench were determined at various temperatures between 20.0 and 55.0 °C. $\langle s^2 \rangle$ was converted to the expansion factor α^2 by using the values of $\langle s^2 \rangle$ at the θ-temperature. The values of α^2 may be subject to an uncertainty of 5% in the measurements. In Figure 3 we plotted α^2 at 30 min after quench against $(1 - \theta/T)M^{1/2}$ for $M_w \times 10^{-6} = 1.57$ (×), 2.84 (○), 4.0 (△), and 12.2 (□) with the open symbols. The data points for $M_w \times 10^{-6} = 1.57$, 2.84, and 4.0 are close to each other and appear to construct a composite curve. The very different behavior of the data points for $M_w = 12.2 \times 10^6$ implies transient expansion factors as demonstrated in Figure 2. In Figure 4 we plotted α^{-3} against $(1 - \theta/T)M^{1/2}$ with the same symbols as in Figure 3 in order to examine the behavior of the data points in the globule region. This plot turns the direction abruptly near the crossover point between globule and coil regions and gives a straight line in the globule region.[19] The solid lines in Figures 3 and 4 are depicted by the same equation for the equilibrium expansion factor as explained later. In Figure 4 the data points in the globule region for $M_w = 1.57 \times 10^6$ can be represented by the straight line, from which the data points for $M_w \times 10^{-6} = 2.84$, 4.0, and 12.2 deviate downward. For $M_w = 12.2 \times 10^6$ the deviation is very large and appears to start near the θ-temperature in Figure 3. Since the deviation suggested a transient expansion factor, we carried out time-resolved light-scattering measurements at selected temperatures to reveal the chain collapse process. For $M_w = 1.57 \times 10^6$, the polymer chain was found to collapse to equilibrium sizes in the first 30 min after quench, because $\langle s^2 \rangle$ determined at 60 min agreed with that at 30 min.

Behavior of Chain Collapse Process. Parts a, b, and c of Table 1 give data of α^2 and M_w obtained by the time-resolved measurements for $M_w \times 10^{-6} = 2.84$, 4.0,

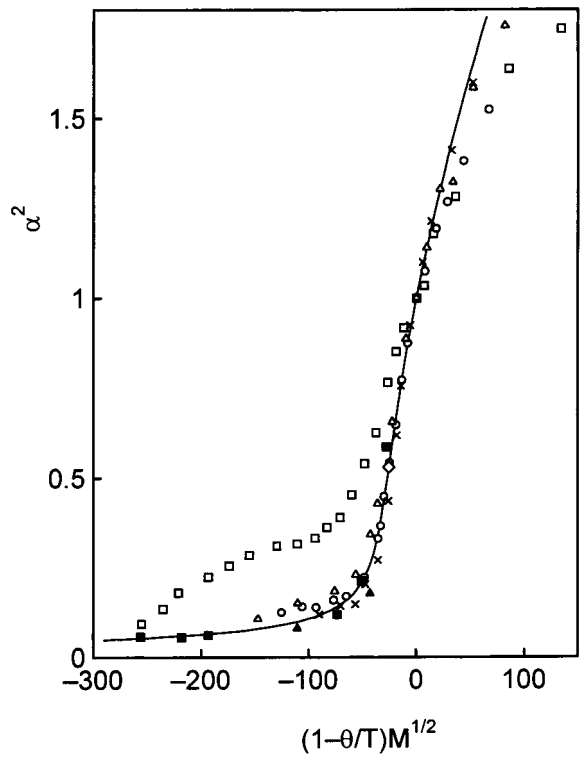

Figure 3. Plot of expansion factor α^2 vs $(1 - \theta/T)M^{1/2}$ for PMMA in the mixed solvent *tert*-butyl alcohol + water (2.5 vol %) with various molecular weights as $M_w \times 10^{-6} = 1.57$ (crosses), 2.84 (circles), 4.0 (triangles), and 12.2 (squares). The open symbols and crosses represent data obtained 30 min after quench. The filled symbols represent α^2_∞ in Table 2. The solid curve is given by eq 3 with $B = 0.0164$ and $C = 0.049$. The diamond represents a crossover point between coil and globule regions.

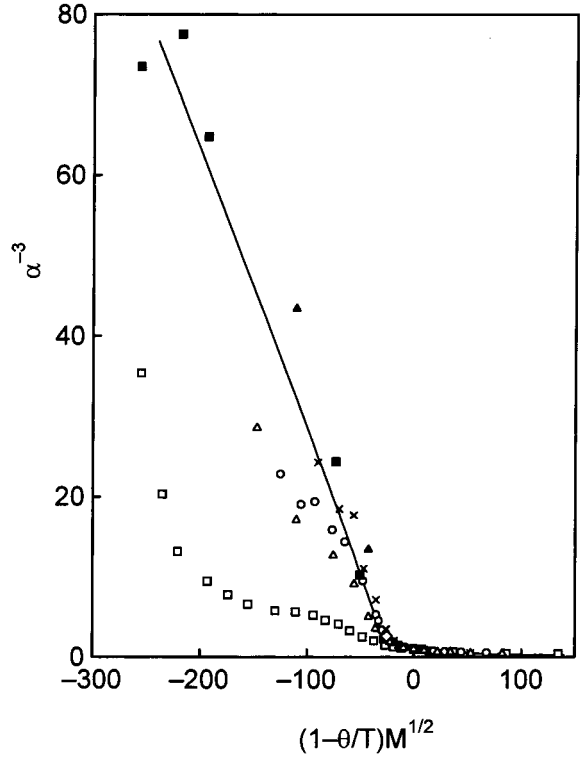

Figure 4. Plot of α^{-3} vs $(1 - \theta/T)M^{1/2}$ for various molecular weights. The symbols and line are the same as in Figure 3.

and 12.2, respectively. The molecular weight indicates a measure for chain aggregation. The measurements were carried out, until fully collapsed chains were observed. For $M_w = 2.84 \times 10^6$, α^2 obtained at 35.0 and 23.0 °C becomes constant within about 60 min after quench. For $M_w = 4.0 \times 10^6$, chain collapse processes are observed clearly for a time period of several hours at 35.0 and 25.0 °C. For both $M_w \times 10^{-6} = 2.84$ and 4.0, α^2 exhibits constant values at 20.0 °C.

For $M_w = 12.2 \times 10^6$, we performed light-scattering measurements for a long time period as indicated by the last data in each column in Table 1c. However, we listed the data that demonstrate the collapse process to a constant value of α^2. Thus, the data after an attainment of the constant value are omitted from Table 1c except for the last ones, which reveal extremely slow phase separations for $M_w = 12.2 \times 10^6$. At 37.0 and 35.0 °C, the observed molecular weight increases appreciably with time, while it is constant at 39.0 °C. The Zimm plots of the light-scattering data at the former two temperatures were not distorted, and accordingly, the slight increase of the apparent molecular weight did not affect the determination of $\langle s^2 \rangle$. The phase separation temperature can be predicted to be between 37.0 and 39.0 °C from the behavior of the apparent molecular weight. This prediction is consistent with that made in the Experimental Section. At 25.0 and 23.0 °C, α^2 reaches constant values about 36 000 min after the quench, and the molecular weight is constant for the whole experimental time period. At 23.0 °C the measurement is extended to 4 months after quench.

The solutions quenched rapidly to 25.0 and 23.0 °C appear to be stable thermodynamically, though the solutions have phase separation temperatures between 37.0 and 39.0 °C. On lowering temperature extremely slowly, the phase separation may occur at a value of α^2. On the other hand, the rapid quench gives rise to the collapse of polymer chains before an onset of chain aggregation. By our intuition the sudden chain collapse may shift the phase separation temperature to lower temperatures because of a smaller chance of contacts between collapsed chains. Therefore, this phenomenon stems from a cooperativity between processes of chain collapse and chain aggregation and cannot be argued quantitatively at present. At 20.0 °C, on the other hand, the polymer chain collapses substantially within the first 30 min after quench and is followed by a very slow contraction process. In accordance with the fast chain collapse in the first 30 min, chain aggregation may start immediately after the collapse as shown by the plot c in Figure 1, which indicates that the chain aggregation occurs stringently on lowering temperature and increasing concentration. In Table 1a,b, the constant α^2 at 20.0 °C implies a rapid collapse to an equilibrium globule within 30 min after quench. Below 20.0 °C the fast chain aggregation was observed irrespective of the molecular weight in the present experimental range of concentration.

Analysis of Observed Chain Collapse Process. Figures 5 and 6 illustrate the chain collapse for $M_w \times 10^{-6} = 4.0$ and 12.2 by plotting α^2 against ln t, respectively, where t is the time in minutes. In Figure 5 the upper and lower plots show the collapse processes at 35.0 and 25.0 °C, respectively. In Figure 6 the plots from top to bottom represent the collapse processes at 39.0, 37.0, 35.0, 25.0, 23.0, and 20.0 °C, respectively. We explored a functional form that could fit the observed collapse processes properly. In this analysis, the equilibrium value α^2_∞ at infinite time was assumed to

Table 1. Time Dependence of the Expansion Factor $\alpha^2 = \langle s^2 \rangle / \langle s^2 \rangle_0$ for Each Molecular Weight[a]

(a) $M_w = 2.84 \times 10^6$

35.0 °C			23.0 °C			20.0 °C		
t (min)	$M_w \times 10^{-6}$	α^2	t (min)	$M_w \times 10^{-6}$	α^2	t (min)	$M_w \times 10^{-6}$	α^2
30	2.87	0.344	30	2.74	0.144	30	2.86	0.110
60	2.86	0.305	60	2.76	0.130	60	2.88	0.109
90	2.89	0.307	90	2.83	0.116	90	2.87	0.108
120	2.97	0.311	120	2.76	0.125	120	2.79	0.111
150	2.89	0.287	180	2.83	0.120	180	2.81	0.110
180	2.93	0.298						

(b) $M_w = 4.0 \times 10^6$

35.0 °C			25.0 °C			20.0 °C		
t (min)	$M_w \times 10^{-6}$	α^2	t (min)	$M_w \times 10^{-6}$	α^2	t (min)	$M_w \times 10^{-6}$	α^2
30	4.25	0.265	30	4.11	0.141	30	4.06	0.101
60	4.13	0.225	60	4.07	0.131	60	4.01	0.104
90	4.18	0.209	90	3.98	0.120	90	4.09	0.094
120	4.07	0.188	120	3.97	0.116	120	4.11	0.094
180	4.24	0.193	180	4.01	0.103	240	4.01	0.095
240	4.13	0.179	240	4.02	0.097	300	4.02	0.104
360	4.23	0.184	300	4.02	0.106			
600	4.32	0.185	360	3.99	0.098			
			420	3.96	0.096			
			660	3.89	0.094			
			1020	3.97	0.083			
			1440	4.02	0.088			

(c) $M_w = 12.2 \times 10^6$

39.0 °C			37.0 °C			35.0 °C		
t (min)	$M_w \times 10^{-6}$	α^2	t (min)	$M_w \times 10^{-6}$	α^2	t (min)	$M_w \times 10^{-6}$	α^2
30	11.7	0.749	30	12.5	0.574	30	12.9	0.382
60	12.1	0.723	60	13.0	0.506	70	13.3	0.308
90	12.6	0.702	90	12.5	0.449	120	13.6	0.269
120	12.1	0.675	120	12.8	0.428	180	13.7	0.242
180	12.4	0.663	180	13.0	0.401	240	13.9	0.227
360	12.8	0.653	240	13.2	0.381	300	13.8	0.215
540	12.5	0.620	300	13.1	0.361	360	13.9	0.208
1260	12.4	0.597	360	13.2	0.349	420	13.9	0.199
1800	12.5	0.603	480	13.5	0.335	540	14.1	0.192
2820	12.2	0.589	600	13.2	0.317	660	14.2	0.185
4560	12.6	0.602	720	13.6	0.306	840	14.3	0.178
33180	12.5	0.596	960	13.5	0.288	1260	14.1	0.163
			1200	13.3	0.275	1740	14.2	0.155
			1440	13.3	0.264	2340	14.3	0.148
			1920	13.6	0.257	2940	14.3	0.143
			2460	14.2	0.255	3660	14.3	0.138
			2880	13.8	0.240	4380	14.4	0.136
			3960	14.2	0.234	5100	14.4	0.130
			4320	14.5	0.235	5820	14.7	0.135
			6480	14.8	0.228	6540	14.5	0.129
			8700	14.7	0.218	7260	14.4	0.128
			10260	14.8	0.216	7980	14.5	0.126
			11700	14.8	0.214	8700	14.7	0.128
			12780	15.3	0.218	9420	14.7	0.125
			14220	15.8	0.223	10140	14.6	0.124
			23040	17.1	0.231	11580	14.5	0.121
						13020	14.8	0.122
						14460	14.9	0.123
						195000	38.1	0.268

Table 1 (Continued)

25.0 °C			23.0 °C			20.0 °C		
t (min)	$M_w \times 10^{-6}$	α^2	t (min)	$M_w \times 10^{-6}$	α^2	t (min)	$M_w \times 10^{-6}$	α^2
30	13.3	0.234	30	13.0	0.156	30	12.4	0.090
60	13.5	0.218	60	13.0	0.144	70	12.4	0.085
90	13.6	0.206	90	13.1	0.138	110	12.4	0.083
120	13.8	0.205	120	13.0	0.132	150	12.5	0.080
180	13.9	0.194	180	13.1	0.125	190	12.1	0.082
240	13.6	0.183	240	13.0	0.124	240	11.9	0.085
360	13.3	0.169	300	13.0	0.122	300	12.0	0.082
480	13.3	0.163	420	12.8	0.113	360	12.0	0.080
720	13.4	0.154	540	13.0	0.111	480		0.080
1080	13.5	0.141	780	13.0	0.105	600		0.080
1440	13.3	0.132	1140	12.7	0.095	1020		0.076
2160	13.4	0.123	1500	12.9	0.095	1800		0.081
2880	13.2	0.113	2160	12.9	0.090	2760		0.075
4320	13.2	0.107	2940	13.0	0.088	4200		0.078
5760	13.5	0.104	4500	12.6	0.081	5640		0.075
7200	13.2	0.092	6300	12.8	0.079	7080		0.072
8640	13.0	0.088	7260	13.0	0.077	9960		0.075
11520	13.3	0.087	8580	12.9	0.076	14280		0.072
14400	13.1	0.081	10080	12.9	0.071	17160		0.071
17220	13.1	0.078	11640	13.0	0.070	20040		0.073
20160	13.0	0.075	12960	13.0	0.071	22920		0.069
23040	13.2	0.076	14820	12.8	0.068	25800		0.063
25980	13.5	0.075	17400	13.0	0.067	30120		0.069
28800	13.2	0.070	21360	13.2	0.070	35880		0.063
31680	13.3	0.070	21780	13.3	0.068	41640		0.059
34560	13.1	0.066	27480	13.1	0.064	47400		0.059
37380	12.9	0.064	29160	13.2	0.065	122040		0.064
40440	13.0	0.067	31440	13.2	0.066			
43260	13.2	0.067	35880	12.7	0.060			
46080	13.1	0.063	41520	13.1	0.059			
48960	13.1	0.064	47640	12.8	0.059			
			178560	13.1	0.059			

[a] The mean-square radius of gyration $\langle s^2 \rangle$ was determined by static light scattering at the time t (min) after quench of solutions to the indicated temperatures. The molecular weight M_w observed at each time is given as a measure of polymer chain aggregation. The values of α^2 may be subject to an uncertainty of 5% in the measurements.

Table 2. Values of α^2_∞, τ^*, and β in Eq 2 for PMMA in the Mixed Solvent *tert*-Butyl Alcohol + Water (2.5 vol %)

	$M_w = 4.0 \times 10^6$		$M_w = 12.2 \times 10^6$					
temp (°C)	35.0	25.0	39.0	37.0	35.0	25.0	23.0	20.0
α^2_∞	0.177	0.081	0.587	0.212	0.119	0.062	0.055	0.057
τ^* (min)	3.19	0.054	42.2	57.2	12.1	0.574	0.017	
β	0.363	0.157	0.358	0.300	0.240	0.122	0.103	
$\langle \tau \rangle^a$ (min)	14.2	78.1	196	530	374	35000	32000	

[a] $\langle \tau \rangle$ is the average characteristic time due to eq 4.

be slightly smaller than the constant value obtained at sufficiently long time after the quench. First, we tried the power law and exponential law to fit the collapse processes, but a satisfactorily agreement was not obtained in the whole experimental ranges of temperature and molecular weight. Next, polynomials were applied for the collapse processes but were not fitted to the data with a small number of terms. However, we found that the stretched exponential function[43] can be fitted to the chain collapse processes in the experimental ranges of temperature and molecular weight. Moreover, since the stretched exponential function seemed to satisfy the initial condition of $\alpha^2 = 1$ at $t = 0$, we analyzed the chain collapse processes by the equation

$$\alpha^2 = \alpha^2_\infty + (1 - \alpha^2_\infty) \exp[-(t/\tau^*)^\beta] \qquad (2)$$

where β and τ^* are constant independent of t. The plot of $\ln \ln[(1 - \alpha^2_\infty)/(\alpha^2 - \alpha^2_\infty)]$ vs $\ln t$ for each process was linear, and the values of β and τ^* were determined unambiguously. Since for the processes at 25.0 and 23.0 °C for $M_w = 12.2 \times 10^6$ data points at small α^2, say $\alpha^2 < 0.1$, deviated from the straight line significantly, the values of β and τ^* were determined with data at larger α^2. At 20.0 °C the obtained difference $\alpha^2 - \alpha^2_\infty$ was not large enough for a reliable determination of β and τ^*, because polymer chains collapsed markedly in the first 30 min. Table 2 gives the obtained values of α^2_∞, β, and τ^*. Figures 7 and 8 represent the plots of $\ln[(\alpha^2 - \alpha^2_\infty)/(1 - \alpha^2_\infty)]$ vs t^β for $M_w \times 10^{-6} = 4.0$ and 12.2 with the values of α^2_∞ and β given in Table 2, respectively, where the symbols are the same as in Figures 5 and 6. For each process the data points are well represented by the straight line, which has the slope $-(1/\tau^*)^\beta$ and passes

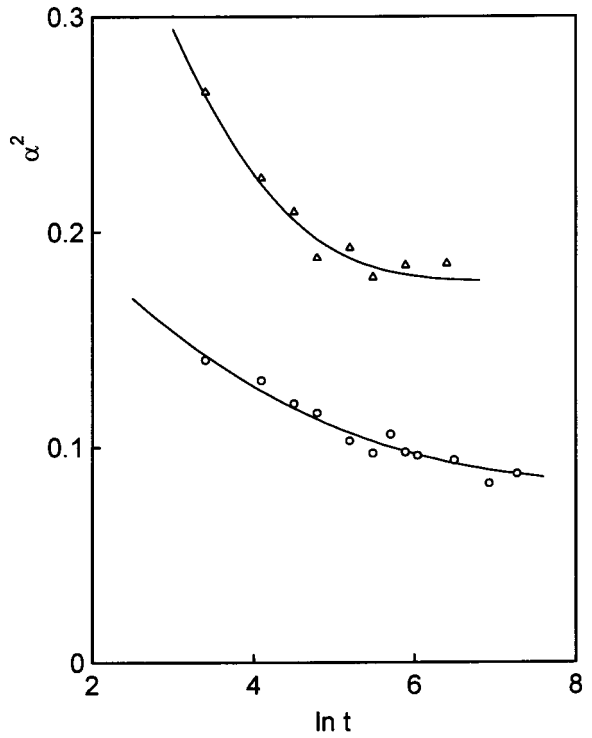

Figure 5. Chain collapse processes for $M_w = 4.0 \times 10^6$ by the plot of α^2 vs ln t with the time t in minutes. The triangles and circles show the processes obtained at 35.0 and 25.0 °C, respectively. The lines are given by eq 2 with the values of α^2_∞, τ^*, and β in Table 2.

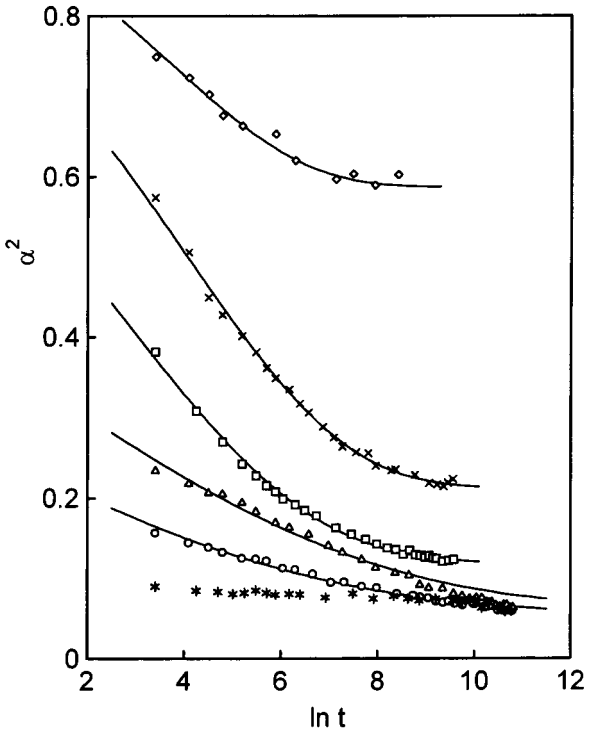

Figure 6. Chain collapse processes for $M_w = 12.2 \times 10^6$ by the same plot as in Figure 5. The diamonds, crosses, squares, triangles, circles, and stars show the processes measured at 39.0, 37.0, 35.0, 25.0, 23.0, and 20.0 °C, respectively. The lines are given by eq 2 with the values of α^2_∞, τ^*, and β in Table 2.

through the origin. At sufficiently large t data points scatter largely because of the vanishing difference $\alpha^2 - \alpha^2_\infty$. Nevertheless, in the processes at 25.0 and 23.0 °C for $M_w = 12.2 \times 10^6$, the data points at large t are

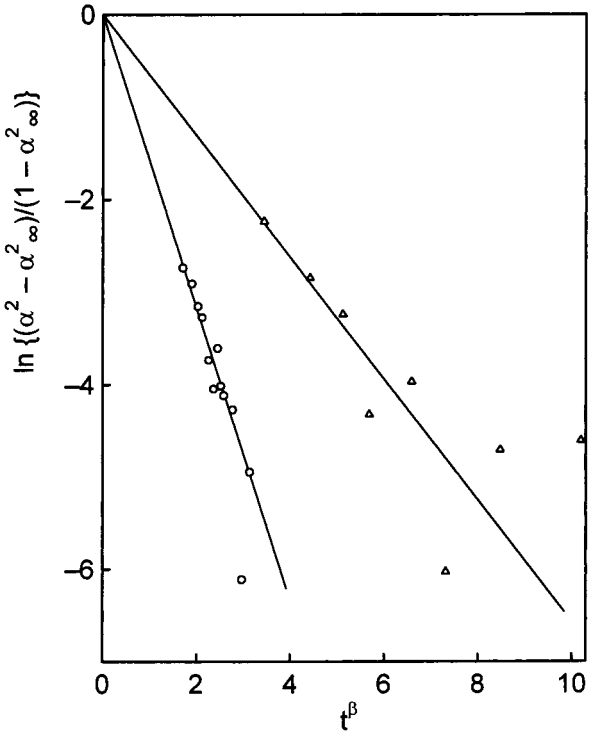

Figure 7. Chain collapse processes for $M_w = 4.0 \times 10^6$ by the plot according to eq 2 with the values of α^2_∞ and β in Table 2. The symbols are the same as in Figure 5.

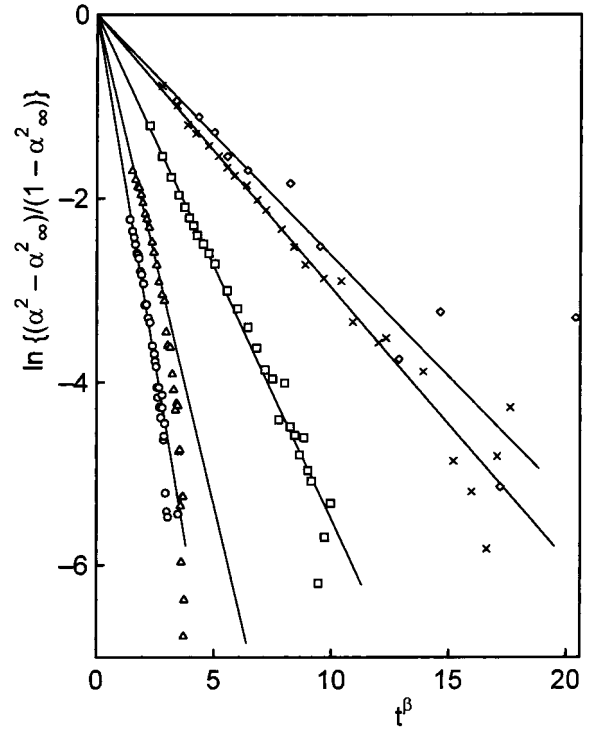

Figure 8. Chain collapse processes for $M_w = 12.2 \times 10^6$ by the plot according to eq 2 with the values of α^2_∞ and β in Table 2. The symbols are the same as in Figure 6.

observed to deviate downward from the straight lines clearly.

As shown in Figure 6, the chain collapse processes at 39.0, 37.0, and 35.0 °C are obtained at relatively large values of α^2 and in a relatively wide range of α^2. These processes are represented by the straight lines passing through the origin in Figure 8 and consequently may

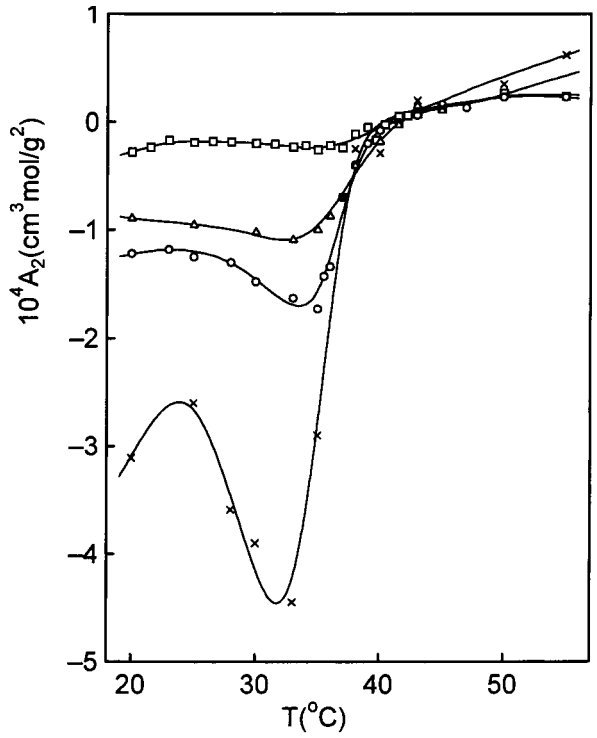

Figure 9. Plot of the second virial coefficient A_2 vs temperature T for data obtained 30 min after quench for various molecular weights as $M_w \times 10^{-6} = 1.57$ (crosses), 2.84 (circles), 4.0 (triangles), and 12.2 (squares).

be compared with a single-stage collapse rather than a two-stage collapse. The earlier processes at 25.0 and 23.0 °C may be caused by the same mechanism as those at the high temperatures, but the later stages may involve another different mechanism of chain collapse. As shown later, the expansion factor at the coil−globule crossover point is estimated as $\alpha^2 = 0.53$. Thus, the chain collapse process at 39.0 °C has been observed in the coil region.

Second Virial Coefficient Observed 30 min after Quench. Figure 9 represents the second virial coefficient A_2 measured 30 min after the quench as a function of temperature for $M_w \times 10^{-6} = 1.57$ (×), 2.84 (○), 4.0 (△), and 12.2 (□). The obtained values of A_2 are affected by the slow chain collapse and chain aggregation. The values of A_2 for $M_w \times 10^{-6} = 1.57$ and 2.84 were measured for fully collapsed chains but may be affected slightly by the chain aggregation due to phase separation. The Zimm plots in Figure 2 give $A_2 = -2.5 \times 10^{-5}$ cm^3 mol/g^2 at 30 min and -5.2×10^{-5} at 178 560 min. However, since these values of A_2 for $M_w = 12.2 \times 10^6$ are very small in magnitude, the relative location of the curves of A_2 vs temperature in Figure 9 may reflect a legitimate molecular weight dependence of A_2. The curves for the three lower molecular weights yield a clear minimum slightly below the coil−globule crossover temperature which is calculated by $(1 - \theta/T)M^{1/2} = -25.6$ as shown later. The minimum decreases with decreasing molecular weight. This behavior of the minimum has been predicted by a theoretical calculation based on a mean-field model with the chain collapse into account[44] and also observed for a solution of polystyrene in cyclohexane.[45] For $M_w \times 10^{-6} = 1.57$ and 2.84, the values of A_2 which were corrected for the effect of phase separation showed essentially the same behavior as those in Figure 9.[18]

4. Discussion and Conclusion

Equilibrium Expansion Factor. Figure 4 and Table 1a show that polymer chains for $M_w \times 10^{-6} = 1.57$ and 2.84 collapse to nearly equilibrium globule within 30 min after the quench. Chain collapse processes were measured for $M_w \times 10^{-6} = 4.0$ and 12.2 for a long time period as shown in Figures 5 and 6, respectively. During the processes we observed the molecular weight to disclose the effect of the chain aggregation. The constant and slowly increasing molecular weights in Table 1 demonstrate that the obtained values of α^2 represent the size of a single polymer chain. Furthermore, we determined the size of the chain with the Zimm plot as in Figure 2, where the lines for the plot of $(Kc/R_\theta)^{1/a}$ vs $\sin^2(\theta/2)$ give a same slope. The aggregation of polymer chains depends on the polymer concentration and, accordingly, may yield lines with different slopes in the Zimm plot. Thus, the observed chain collapse process represents the behavior of a single polymer chain. This was also the case in the previous study for PMMA in isoamyl acetate.[38] In the study we did not observe a formation of small clusters of several polymer chains but determined the chain collapse process of single polymer chains.[46,47]

In previous studies,[18,19] the expansion factor determined below the θ-temperature was compared with a mean-field theory for a contracted chain ($\alpha^2 < 1$) given by[9]

$$\alpha^3 - \alpha - C(\alpha^{-3} - 1) = B(1 - \theta/T)M^{1/2} \qquad (3)$$

where B and C are constants associated with the second and third virial coefficients for segment interactions, respectively. According to eq 3, the plot of $(\alpha^3 - \alpha)/(\alpha^{-3} - 1)$ vs $(1 - \theta/T)M^{1/2}/(\alpha^{-3} - 1)$ for data in the range $\alpha^2 < 1$ should be linear, and the slope and intercept of the line yield B and C, respectively. The plot, which was made with the data of α^2 for $M_w \times 10^{-6} = 1.57$ and 2.84, yielded a well-defined straight line, from which $B = 0.0164$ and $C = 0.049$ were determined. These values agree with those of $B = 0.0160$ and $C = 0.044$ determined previously.[18] In Figures 3 and 4 the solid lines are given by eq 3 with the present values of B and C. The values of α^2_∞ in Table 2 are given by the filled symbols corresponding to the open symbols to specify the molecular weight. Since the filled symbols come close to the solid lines in Figures 3 and 4, α^2_∞ in Table 2 is found to give equilibrium expansion factors. The coil−globule crossover point was assumed to coincide with an inflection point on the curve of α^2 vs $(1 - \theta/T)M^{1/2}$ and was calculated as $\alpha^2 = 0.53$ and $(1 - \theta/T)M^{1/2} = -25.6$ by using eq 3. This crossover point is given by the open diamond in Figures 3 and 4 and has been shown to agree with that estimated by a theoretical consideration.[10,19] In Figure 4, the globule state appears to be represented by a straight line.

Chain Collapse Process. The stretched exponential function has been widely used to describe relaxation behavior of various phenomena in glass-forming liquids and amorphous polymers.[48,49] The nonexponential relaxation can be obtained by a superposition of exponentially relaxing processes with various relaxation times and has been explained as an evidence of inhomogeneity in complex systems.[50] On the other hand, Ngai and coworkers interpreted the nonexponential behavior by cooperative interactions between relaxing units: the coupling of relaxing units causes a slowdown of the

relaxation and yields the stretched exponential behavior.[51]

The observed chain collapse process is different from relaxation phenomena in complex systems such as bulk polymers.[49] However, the above arguments on the relaxation phenomena suggest two phenomenological interpretations for the chain collapse process. First, isolated polymer chains can be assumed to undergo exponentially collapsing processes with different characteristic times τ. Then, the stretched exponential function could be observed as a superposition of the various exponential processes. The average characteristic time $\langle\tau\rangle$ is given by[50]

$$\langle\tau\rangle = (\tau^*/\beta)\Gamma(1/\beta) \tag{4}$$

where $\Gamma(1/\beta)$ is the gamma function. It should be noticed that $\langle\tau\rangle$ can be calculated from τ^* and β without resorting to a distribution of τ. For $\beta = 1$, eq 4 gives $\langle\tau\rangle = \tau^*$ in accordance with eq 2. With decreasing β the distribution of τ becomes wider.[50] The values of $\langle\tau\rangle$ calculated by eq 4 are given in Table 2. In light of Table 1b,c, the values of $\langle\tau\rangle$ do not seem to contradict with the experimental time period for the chain collapse. The behavior of β in Table 2 would imply that the distribution of τ becomes wider with decreasing temperature. This temperature dependence of β, i.e., the width of the distribution of τ, cannot be explained by the molecular weight distribution, which does not depend on temperature. The much smaller values of β than unity in Table 2 mean a very wide distribution of τ.[50] It seems to be difficult to find out a plausible reason for the distribution of τ and its strong temperature dependence.

In the second description of chain collapse, each polymer chain is assumed to undergo a collapse due to the stretched exponential. A phenomenological expression for the process is written in the differential form

$$d\alpha^2/dt = -W(t)\alpha^2 \tag{5}$$

where the collapse rate $W(t)$ depends on time as $At^{\beta-1}$. In this description, it is relevant to mention an effect of the mixed solvent *tert*-butyl alcohol + water (2.5 vol %) on the chain collapse process. Pure *tert*-butyl alcohol is a nonsolvent for PMMA, and an addition of a small amount of water increases the solvent power drastically. Thus, the mixed solvent is a cosolvent for PMMA.[52] In the chain collapse process, the fraction of water in a polymer domain may change depending on α^2 and appears to influence the rate of chain collapse. However, the preferential sorption in the mixed solvent does not seem to be large enough to explain the small value of β and its large temperature dependence. According to an argument by Cowie et al., the preferential sorption is not a main cause of the cosolvency of the mixed solvent.[52] Preferential sorptions determined by static light scattering are usually very small even in cosolvent systems.[53]

In Table 1c, the chain collapse at 20.0 °C is seen to occur substantially in the first 30 min, which suggests a very small value of β. Equation 5 with $\beta = 0$ suggests a power law collapsing process. In the previous study for PMMA in the single solvent of isoamyl acetate, we obtained the power law collapsing process expressed by[38]

$$\alpha^2 = \alpha^2_\infty + \{b/(t + c)\}^p \tag{6}$$

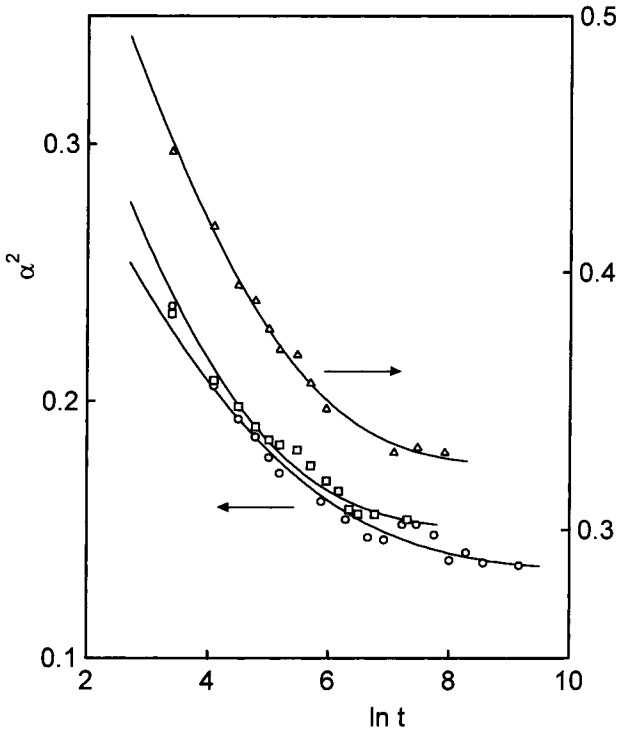

Figure 10. Chain collapse processes by the plot of α^2 vs ln t with the time t in minutes for PMMA in isoamyl acetate.[38] The circles and triangles show the processes obtained at 30.0 and 45.0 °C for $M_w = 12.2 \times 10^6$, respectively. The squares show the process at 30.0 °C for $M_w = 8.4 \times 10^6$. The lines are given by eq 2 with the values of α^2_∞, τ^*, and β in Table 3.

Table 3. Values of α^2_∞, τ^*, and β in Eq 2 for PMMA in Isoamyl Acetate[38]

	$M_w = 8.4 \times 10^6$	$M_w = 12.2 \times 10^6$	
temp (°C)	30.0	45.0	30.0
α^2_∞	0.150	0.325	0.134
τ^* (min)	0.878	4.12	0.267
β	0.228	0.261	0.169
$\langle\tau\rangle^a$ (min)	38.3	77.0	165
$\alpha^2_\infty{}^b$	0.142	0.308	0.131

[a] $\langle\tau\rangle$ is the average characteristic time due to eq 4. [b] Determined by eq 6.

where b, c, and p were constants independent of time and were determined under the initial condition $\alpha^2 = 1$ at $t = 0$. We analyzed the previous data by eq 2 and obtained a fairly good agreement between eq 2 and the data as shown in Figure 10. The values of α^2_∞, β, τ^*, and $\langle\tau\rangle$ are given in Table 3. It is seen that β decreases with decreasing temperature and with increasing molecular weight. This behavior is in accord with that for the present system. The values of α^2_∞ determined with eq 2 are in a good agreement with the previous ones due to eq 6. For lack of data in the first 30 min, the observed collapse processes appeared to be described equally well by the power law and stretched exponential function. However, it should be noticed that eq 2 can be fitted to the data points with a smaller number of parameters than eq 6. Thus, the data obtained with the mixed solvent and with the single solvent suggest that the stretched exponential process may be more common than the power law process, which may occur in limited ranges of temperature and molecular weight. The crossover between the two different processes can be disclosed by precise measurements started immediately after quench in a range where observed β tends to

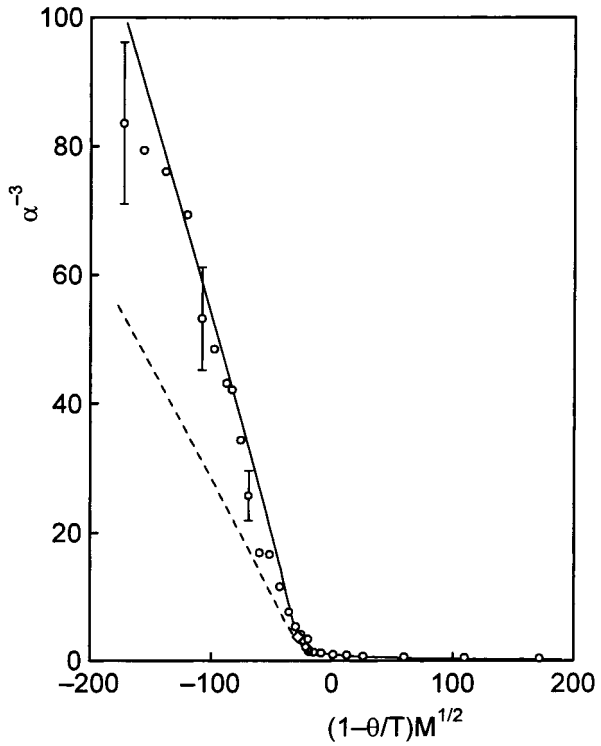

Figure 11. Plot of α^{-3} vs $(1 - \theta/T)M^{1/2}$ for polystyrene in cyclohexane with $M_w = 2.6 \times 10^7$. The data points were read from Figure 2 in ref 12. The vertical bar indicates an error of 5% in α^2. The solid line is described by eq 3 with $B = 0.0162$ and $C = 0.026$. The broken line represents the behavior of the present data for PMMA. The open diamond gives the crossover point between coil and globule regions.

vanish. Computer simulations revealed different stages in a chain collapse process but did not predict a stage of chain collapse due to stretched exponential.[29]

Comparison between Chain Collapses of Different Polymers. Tanaka et al.[12] carried out light-scattering measurements on extremely dilute solutions of polystyrene in cyclohexane with $M_w = 2.6 \times 10^7$ and presented the first experimental data on the coil−globule transition, which were compared with the theoretical prediction by Sanchez.[8] The measurements were made above the phase separation temperature in the concentration range from 3×10^{-8} to 3×10^{-6} g/cm^3. Chu et al. measured a chain collapsing process of polystyrene in cyclohexane with $M_w = 8.1 \times 10^6$ for a time period of several minutes.[34] In light of this observation for chain collapse process, it is important to ascertain whether Tanaka et al. obtained values of α^2 of fully collapsed chains or the transient values in a chain collapse process. We read values of the radius of gyration from Figure 2 in ref 12 by a digital scanner and reproduced the behavior by plotting α^{-3} against $(1 - \theta/T)M^{1/2}$ in Figure 11. The vertical bar indicates a conceivable error of 5% in α^2. The data points are well fitted to the solid line described by eq 3 with $B = 0.0162$ and $C = 0.026$, which were determined by the method described below eq 3. The open diamond represents a coil−globule crossover point determined as an inflection point on the curve of α^2 vs $(1 - \theta/T)M^{1/2}$. The transition from coil state to globule state appears to occur abruptly. On account of the interpretation of the plot in Figure 4, the agreement between the data points and the solid line in Figure 11 indicates that the data have been obtained for fully collapsed chains. Since Tanaka et al. seemed to carry out the experiment without paying attention to the time period of chain collapse, we suppose that the light-scattering measurement was performed within a few hours after the quench of solution as in usual experiments. Thus, polystyrene chains in cyclohexane may collapse rapidly to the equilibrium globule even for the very high molecular weight $M_w = 2.6 \times 10^7$. Tanaka et al.[11] determined the phase separation temperature in the very low concentration range from 10^{-8} to 10^{-3} g/cm^3 by monitoring scattered intensities which increased due to an aggregation of polymer chains. According to this experiment, the chain aggregation occurs fast in the polystyrene solution at the low concentration even for $M_w = 2.6 \times 10^7$, in contrast to the slow chain aggregation in the present solutions of PMMA.

Wang et al.[54] determined the expansion factors for radius of gyration and for hydrodynamic radius for PNIPAM with $M_w = 1.3 \times 10^7$. Both the expansion factors were represented by eq 3 in the coil region and had constant values independent of temperature in the globule region. In the coil region the coefficients in eq 3 were determined as $B = 0.0379$ and $C = 0.008\,54$ for radius of gyration and $B = 0.0325$ and $C = 0.0295$ for hydrodynamic radius, which gave the ratios $C/B = 0.225$ and 0.908, respectively. This large difference could not be explained reasonably.

For the present system of PMMA in the mixed solvent, we obtained $B = 0.0164$ and $C = 0.049$, which give the broken line in Figure 11. Equation 3 has a critical point for $C = 0.005\,49$, below which the chain collapse occurs discontinuously. The values of C obtained for polystyrene and PMMA are much larger than the critical value, while the value of $C = 0.008\,54$ for PNIPAM is close to the critical one and reflects a narrow temperature region of transition. The globule state $\alpha^{-3} \sim (1 - \theta/T)M^{1/2}$ obtained for PMMA and polystyrene is in marked contrast to the globule state $\alpha^3 \sim$ constant for PNIPAM. The segment mass concentration in a globule may be given by $c_s = (M/N_A)/[(4\pi/3)\kappa\langle s^2\rangle^{3/2})]$ with $\kappa = (5/3)^{3/2}$. For PNIPAM the constant value of the radius of gyration yield $c_s = 0.34$ g/cm^3. For PMMA and polystyrene the maximum concentration attained experimentally is estimated as $c_s = 0.21$ and 0.06 g/cm^3, respectively. Wang et al. suggested that the large value of $c_s = 0.34$ g/cm^3 was close to a limiting value at the globule state in accordance with the observed constant expansion factors. According to eq 3, the asymptotic behavior in the globule region is given by $\alpha^3 \sim (C/B)/(1 - \theta/T)M^{1/2}$ and $c_s \sim (B/C)(1 - \theta/T)$. Thus, the ratio C/B dominates the segment concentration in a globule. For PMMA and polystyrene, C/B is estimated to be respectively 2.9 and 1.6, which are larger than those for PNIPAM.

DNA has been known to undergo a discontinuous coil−globule transition, indicating a small value of C in eq 3.[7] Although a recent direct observation by fluorescence images visualized the discontinuous transition of DNA,[55] the kinetics of the transition has not been studied. We suppose that the collapse of DNA might be too fast to be followed by an experiment.

The coil−globule transitions for the solutions of PMMA, PNIPAM, and polystyrene have a common feature due to eq 3. It is not certain whether the chain collapse process observed for the PMMA solutions may reflect a universal feature characteristic of linear polymer chains or not. However, it is obvious that the rate of a chain collapse is due to a specific nature of solution

and cannot be predicted from the conventional solution properties. The segment concentration in a globule does not seem to be of primary importance for the chain collapse process.

Chain Collapse and Chain Aggregation. In a preceding paper,[56] we studied chain aggregation processes for solutions of PMMA with $M_w = 1.57 \times 10^6$ in the mixed solvent *tert*-butyl alcohol + water (2.5 vol %) at 25.0 and 30.0 °C by static light scattering. The observed chain aggregation process was very slow and expressed by an exponential function in the initial stage. Thus, the process was attributed to the reaction-limited cluster aggregation (RLCA) rather than the diffusion-limited cluster aggregation (DLCA).[41] The aggregation process was relatively faster at 30.0 °C than at 25.0 °C and was compatible with the behavior of A_2, which exhibits a minimum near 30.0 °C and a maximum near 25.0 °C in Figure 9. The chain collapse and chain aggregation processes may be dominated by a specific nature of the polymer segment and solvent, and consequently the rates of the processes are correlated intimately with each other. Thus, the observed slow chain collapse as well as the slow chain aggregation may be caused by the RLCA of polymer segments. It is interesting to elucidate the specific mechanism of the segment aggregation. The chain collapse and chain aggregation in polystyrene solution occur much faster than those in PMMA solution, though the aggregation process of polystyrene chains is too slow to be explained by DLCA.[57]

References and Notes

(1) Grosberg, A. Y.; Khokhlov, A. R. *Statistical Physics of Macromolecules*; AIP Press: New York, 1994.
(2) Grosberg, A. Y.; Khokhlov, A. R. *Giant Molecules*; Academic Press: New York, 1997.
(3) Stockmayer, W. H. *Makromol. Chem.* **1960**, *35*, 54.
(4) Ptitsyn, O. B.; Kron, A. K.; Eizner, Y. Y. J. *Polym. Sci., Part C* **1968**, *16*, 3509.
(5) de Gennes, P. G. *J. Phys., Lett.* **1975**, *36*, L55.
(6) Lifshitz, I. M.; Grosberg, A. Y.; Khokhlov, A. R. *Rev. Mod. Phys.* **1978**, *50*, 683.
(7) Post, C. B.; Zimm, B. H. *Biopolymers* **1979**, *18*, 1487.
(8) Sanchez, I. C. *Macromolecules* **1979**, *12*, 980.
(9) Birshtein, T. M.; Pryamitsyn, V. A. *Macromolecules* **1991**, *24*, 1554.
(10) Grosberg, A. Y.; Kuznetsov, D. V. *Macromolecules* **1992**, *25*, 1970; **1992**, *25*, 1980; **1992**, *25*, 1991.
(11) Swislow, G.; Sun, S. T.; Nishio, I.; Tanaka, T. *Phys. Rev. Lett.* **1980**, *44*, 796.
(12) Sun, S. T.; Nishio, I.; Swislow, G.; Tanaka, T. *J. Chem. Phys.* **1980**, *73*, 5971.
(13) Park, I. H.; Wang, Q. W.; Chu, B. *Macromolecules* **1987**, *20*, 1965.
(14) Chu, B.; Park, I. H.; Wang, Q. W.; Wu, C. *Macromolecules* **1987**, *20*, 2833.
(15) Stepanek, P.; Konak, C.; Sedlacek, B. *Macromolecules* **1982**, *15*, 1214.
(16) Kubota, K.; Fujishige, S.; Ando, I. *J. Phys. Chem.* **1990**, *94*, 5154.
(17) Wu, C.; Zhou, S. *Macromolecules* **1995**, *28*, 8381.
(18) Nakata, M. *Phys. Rev. E* **1995**, *51*, 5770.
(19) Nakata, M.; Nakagawa, T. *Phys. Rev. E* **1997**, *56*, 3338.
(20) Baysal, B. M.; Kayaman, N. J. *Chem. Phys.* **1998**, *109*, 8701.
(21) Wang, X.; Qiu, X.; Wu, C. *Macromolecules* **1998**, *31*, 2972.
(22) Kayaman, N.; Gurel, E. E.; Baysal, B. M.; Karasz, F. E. *Polymer* **2000**, *41*, 1461.
(23) Gurel, E. E.; Kayaman, N.; Baysal, B. M.; Karasz, F. E. *J. Polym. Sci., Part B: Polym. Phys.* **1999**, *37*, 2253.
(24) de Gennes, P. G. *J. Phys., Lett.* **1985**, *46*, L-639.
(25) Grosberg, A. Y.; Nechaev, S. K.; Shakhnovich, E. I. *J. Phys. (Paris)* **1988**, *49*, 2095.
(26) Grosberg, A. Y.; Kuznetsov, D. V. *Macromolecules* **1993**, *26*, 4249.
(27) Ma, J.; Straub, J. E.; Shakhnovich, E. I. *J. Chem. Phys.* **1995**, *103*, 2615.
(28) Byrne, A.; Kiernan, P.; Green, D.; Dawson, K. A. *J. Chem. Phys.* **1995**, *102*, 573.
(29) Kuznetsov, Y. A.; Timoshenko, E. G.; Dawson, K. A. *J. Chem. Phys.* **1995**, *103*, 4807.
(30) Kuznetsov, Y. A.; Timoshenko, E. G.; Dawson, K. A. *J. Chem. Phys.* **1996**, *104*, 3338.
(31) Klushin, L. I. *J. Chem. Phys.* **1998**, *108*, 7917.
(32) Halperin, A.; Goldbart, P. M. *Phys. Rev. E* **2000**, *61*, 565.
(33) Yu, J.; Wang, Z.; Chu, B. *Macromolecules* **1992**, *25*, 1618.
(34) Chu, B.; Ying, Q.; Grosberg, A. Y. *Macromolecules* **1995**, *28*, 180.
(35) Wu, C.; Zhou, S. *Macromolecules* **1995**, *28*, 8381.
(36) Zhu, P. W.; Napper, D. H. *J. Chem. Phys.* **1997**, *106*, 6492.
(37) Zhu, P. W.; Napper, D. H. *Phys. Rev. E* **2000**, *61*, 6866.
(38) Nakata, M.; Nakagawa, T. *J. Chem. Phys.* **1999**, *110*, 2703.
(39) Nakata, M.; Nakagawa, T.; Nakamura, Y.; Wakatsuki, S. *J. Chem. Phys.* **1999**, *110*, 2711.
(40) Nakagawa, T.; Nakamura, Y.; Sasaki, N.; Nakata, M. *Phys. Rev. E* **2001**, *63*, 031803.
(41) Vicsek, T. *Fractal Growth Phenomena*, 2nd ed.; Word Scientific: Singapore, 1992.
(42) Nakata, M. *Polymer* **1997**, *38*, 9.
(43) Williams, G.; Watts, D. C. *Trans. Faraday Soc.* **1970**, *66*, 80.
(44) Tanaka, F. *J. Chem. Phys.* **1985**, *82*, 4707.
(45) Nierlich, M.; Cotton, J. P.; Farnoux, B. *J. Chem. Phys.* **1978**, *69*, 1379.
(46) Kayaman, N.; Gurel, E. E.; Baysal, B. M.; Karasz, F. E. *Macromolecules* **1998**, *32*, 8399.
(47) Raos, G.; Allegra, G. *J. Chem. Phys.* **1997**, *107*, 6479.
(48) Williams, G. J. *Non-Cryst. Solids* **1991**, *131−133*, 1.
(49) Boese, D.; Kremer, F. *Macromolecules* **1990**, *23*, 829.
(50) Lindsey, C. P.; Patterson, G. D. *J. Chem. Phys.* **1980**, *73*, 3348.
(51) Ngai, K. L.; Wang, C. H.; Fytas, G.; Plazek, D. L.; Plazek, D. J. *J. Chem. Phys.* **1987**, *86*, 4768.
(52) Cowie, J. M. G.; Mohsin, M. A.; McEwen, I. J. *Polymer* **1987**, *28*, 1569.
(53) Strazielle, C. Light Scattering in Mixed solvents. In *Light Scattering from Polymer Solutions*; Huglin, M. B., Ed.; Academic Press: London, 1972; p 633.
(54) Wang, X.; Qiu, X.; Wu, C. *Macromolecules* **1998**, *31*, 2972.
(55) Yoshikawa, K.; Takahashi, M.; Vasilevskaya, V. V.; Khokhlov, A. R. *Phys. Rev. Lett.* **1996**, *76*, 3029.
(56) Nakamura, Y.; Nakagawa, T.; Sasaki, N.; Yamagishi, A.; Nakata, M. *Macromolecules* **2001**, *34*, 5984 (preceding paper).
(57) Chuang, J.; Grosberg, A. Yu.; Tanaka, T. *J. Chem. Phys.* **2000**, *112*, 6434.

MA010063H